# INTERPRETATION OF HMC IMAGES BY A COMBINED THERMAL AND GASDYNAMIC MODEL

J. KNOLLENBERG and E. KÜHRT
*Deutsche Forschungsanstalt für Luft- und Raumfahrt,*
*Institut für Weltraumsensorik,*
*Rudower Chaussee 5, 12489 Berlin, Germany*

and

H.U. KELLER
*Max-Planck-Institut für Aeronomie, 37191 Katlenburg-Lindau, Germany*

**Abstract.** Images of comet Halley's nucleus taken by the HMC camera during the GIOTTO encounter in 1986 show that a major part of the total dust production is localized in a few active areas which are the sources of gas-dust jets. The global dust distribution in the inner coma is dominated by two main jets roughly directed to the sun. A combination of a 1D thermal nucleus model with an axisymmetric continuum model of the jet outflow was used to investigate the properties of the inner coma. Detailed investigations show that the characteristics of the observed jets can be reproduced by outgassing from free sublimating active areas of a few km in diameter, a dust to gas ratio of 1 – 2.5 and a size distribution dominated by the larger grains. It is further shown that most of the observational constraints provided by the HMC data can be met simultaneously by a model of three jets superimposed on a weak background.

## 1. Introduction

The spacecraft fly-bys of Halley's comet in 1986 have demonstrated that the dynamics and optical appearance of the inner coma is dominated by jets of gas and dust (Keller *et al.*, 1986; Sagdeev *et al.*, 1987). Images taken by the HMC camera showed that most of the dust production is localized in three active areas which did not cover more than about 20% of the illuminated surface (Keller *et al.*, 1987). These areas are the source regions of the observed gas-dust jets. Reitsema *et al.* (1989) showed that the angular dependence of the intensity can be well described by the sum of three Gaussians and a constant. The halfwidths of the two main jets visible in the HMC images were determined to 31° and 37° (Keller *et al.*, 1994). In spite of the observation that the jets are roughly directed to the sun and that no clear evidence for nightside activity could be detected in the images, a surprisingly high level of intensity was measured on the antisunward side of the images. The ratio of the total intensities integrated over the sunward and antisunward hemispheres was determined to $D/N = 3.2$ (Keller and Thomas, 1989). On the other hand, the jump of the intensity across the nightside terminator was only about a factor of 2–2.5, thus providing evidence against the hypothesis that a jet directed away from HMC could be responsible for the low $D/N$-value observed.

*Earth, Moon, and Planets* **72**: 103-112, 1996.

Because existing jet models suffer from unrealistic assumptions, like a dust concentration in $\mu$m-sized grains [e.g. Kitamura (1987); Körösmezey and Gombosi (1990)] or a large nightside production (Kitamura, 1986), they are not able to explain the observations. Therefore, the objective of this paper is to present a new cometary jet model and to give a quantitative interpretation of the HMC images. Because reliable information about the position and extent of the active regions and of the three-dimensional dust distribution could not be deduced from the measurements, it was decided to develop a new axisymmetric model.

## 2. Model

The physical model of the inner coma can be described by the expansion of a mixture of gas and dust emanating from active regions on the nucleus surface into a vacuum or a radial background flow. The gas phase is characterized by a constant adiabatic exponent $\gamma_{\rm ad} = 4/3$ (corresponding to water vapour) and is treated as an inviscid, compressible continuum.

At the nucleus surface a gas production rate was prescribed as a function of the polar angle $\Theta$ with respect to the jet axis:

$$Z(\Theta) = Z_j f(\Theta) + Z_b. \tag{1}$$

Two extreme cases for the spatial distribution of the production rate inside the active region were considered, a constant [$f(\Theta) = 1$ for $\Theta < \Theta_j$, $f(\Theta) = 0$ otherwise] and a Gaussian distribution of production rate [$f(\Theta) = \exp(-(\Theta/\Theta_j)^2)$]. The actual values of the outgassing rates were calculated using a sophisticated thermal model described in detail by Kührt and Keller (1994). The thermal calculations were carried out for the orbit of P/Halley, a heliocentric distance of 0.89 AU, a rotation period of 55 h and different values of the thermal conductivity of the dust crust in the range $K_c = 0 - 1$ W K$^{-1}$ m$^{-1}$. This model provides the gas flux as a function of latitude and local time but for values of $K_c > 0.1$ W K$^{-1}$ m$^{-1}$ the background production $Z_b$ could be reasonably approximated by a constant. The deviations from isotropic outgassing were less than 15% in these cases. Experiments with different rotation periods showed that $Z_b$ is not critically dependent on the rotational state of the nucleus. The gas production rate on the jet axis was determined by the energy balance of a freely sublimating icy surface to $Z_j = 2\,10^{22}$ mol. m$^{-2}$ s$^{-1}$. The symmetry conditions were used on the axes, for $\Theta = 0°$ and $\Theta = 180°$ and the free outflow conditions were applied at the outer boundary.

The results presented below were calculated with a grain size distribution which was approximated by 11 logarithmically spaced discrete grain sizes between 1 $\mu$m and 1 mm. The grains are considered as spheres with a density of 1 g cm$^{-3}$ and their interaction with the surrounding gas stream is described by the theory of free molecular flow (Hayes and Probstein, 1959). The distribution of mass between the different size classes is characterized by an exponent $\gamma$. The contribution of the individual size classes to the total mass loading $\kappa$ is then given by :

$$\kappa_i = \kappa_m \left(\frac{a_i}{a_m}\right)^{3-\gamma} \tag{2}$$

where $a_m$ and $\kappa_m$ are the radius and the dust to gas ratio of the largest grains.

The numerical solution of the coupled hyperbolic system of conservation laws of gas and dust flow is achieved by an explicit second order Godunov-type scheme. The continuum equations were integrated in time until a steady state was reached. Calculations were performed on a fixed grid of $180 \times 51$ points with an angular spacing of $\Delta\Theta = 1°$ and an increasing radial mesh size with distance from the nucleus. The nucleus is assumed to be spherical with a radius of $R_N = 6$ km. The width of the first computational cell above the nucleus was 0.1 km and the outer boundary was set at a cometocentric distance of 180 km. A more detailed description of the numerical procedure is given by Knollenberg (1994).

For a direct comparison of the model results with the HMC images the calculated density values were converted to relative intensities by integrating along the line of sight and weighting appropriately with the particle cross sections. Under the assumptions of an optically thin coma (e.g. Chick and Gombosi, 1992) and identical scattering phase functions for all grain size classes, this quantity is proportional to the intensity of the light scattered by the dust grains in the coma.

## 3. Results

Several model runs were performed to study the influence of the dust to gas ratio, the grain size distribution, the extent of the active region and the thermal conductivity of the dust crust on the formation of dust jets. Furthermore, the influence of the viewing geometry on the optical appearance of the inner dust coma was investigated.

Fig. 1 shows contours of the calculated intensity of two models, both with $\Theta_j = 15°$, a dust to gas ratio $\kappa = 1$ and a size distribution exponent $\gamma = 2.5$ for three different aspect angles (angle jet axis-observer) $\phi = 90°, 107°$ and $135°$. The spherical nucleus is located in the centre and the jet axis is the negative $x$-direction. The contours on the left (Fig. 1a, c and e) were calculated with a thermal conductivity $K_c = 0$ implying a diminishing background production. In this case a smooth decrease from the maximum in the centre to the wings of the jet is obvious (Fig. 1a). This is caused by the strong lateral expansion of the gas jet into the vacuum until the maximum expansion angle is reached (see Koppenwallner *et al.*, 1986). But because the dust particles decouple from the gas flow a few km above the nucleus the dust jet is more confined and no significant flow of grains across the terminator is generated, thus giving a value of $D/N = \infty$. A close inspection reveals that the angular dependence of the intensity can be approximated by a Gauss-function (Knollenberg, 1994).

The results in the right column (Fig. 1b, d and f) were calculated with a thermal conductivity of the crust of $K_c = 0.2\ \mathrm{W\,m^{-1}\,K^{-1}}$, resulting in a background production of $Z_b = 0.2\%$ of $Z_j$. In this case the lateral expansion of the gas is stopped by the ambient pressure in a contact discontinuity. The angular position of the contact surface is determined by the ratio of the gas production rate inside the active region to that of the background. In our example it forms an angle of 80° with the axis. Furthermore, dust is accumulated here, thus forming the narrow cone visible in Fig. 1b. By tracing test particles in the calculated gas flow field, it can be shown that the majority of the dust which is concentrated in this cone stems from an annulus immediately surrounding the active region. On the nightside of the nucleus the undisturbed radial background flow is evident. The low gas production rate causes considerably lower dust particle velocities compared with the velocities assumed on the jet axis (by a factor of 6–15, depending on the grain size). Thus, a surprisingly high intensity is apparent in the antisunward hemisphere and a ratio of $D/N = 2.3$ results.

In Figure 1 c–f, the effect of a changing aspect angle on the optical appearance of the inner dust coma is demonstrated. For the isolated jet with no background production the shape of the contours remains, but they are slightly broadened and some dust appears in projection on the antisunward side of the nucleus. For $\phi = 135°$ a value of $D/N = 25$ is reached and the jump in intensity by crossing the nightside limb is $I_\infty/I_c = 10^4$ ($I_c$ = intensity just above the nucleus surface). In the case of the surrounded jet a deviation of the aspect angle from 90° causes the narrow dust cone to develop into a broad maximum (Fig. 1d). A further increase then smears out the dust cone completely. The sunward to antisunward ratio remains fairly constant in this range of aspect angles, varying only between $D/N = 2.2 - 2.5$. The intensity jump can be evaluated to be $I_\infty/I_c = 2.7$ for $\phi = 107°$ (corresponding to an exactly sunward jet in the HMC images). Then it is more rapidly increasing with increasing aspect angle, reaching a value of $I_\infty/I_c = 6$ for $\phi = 135°$.

Because the strength of the gas-dust interaction is mainly determined by the total cross section of the dust particles, a variation of the dust/gas ratio $\kappa$ and of the size distribution exponent $\gamma$ has consequences for the resulting halfwidths of the jets. For the same model as discussed above the influence

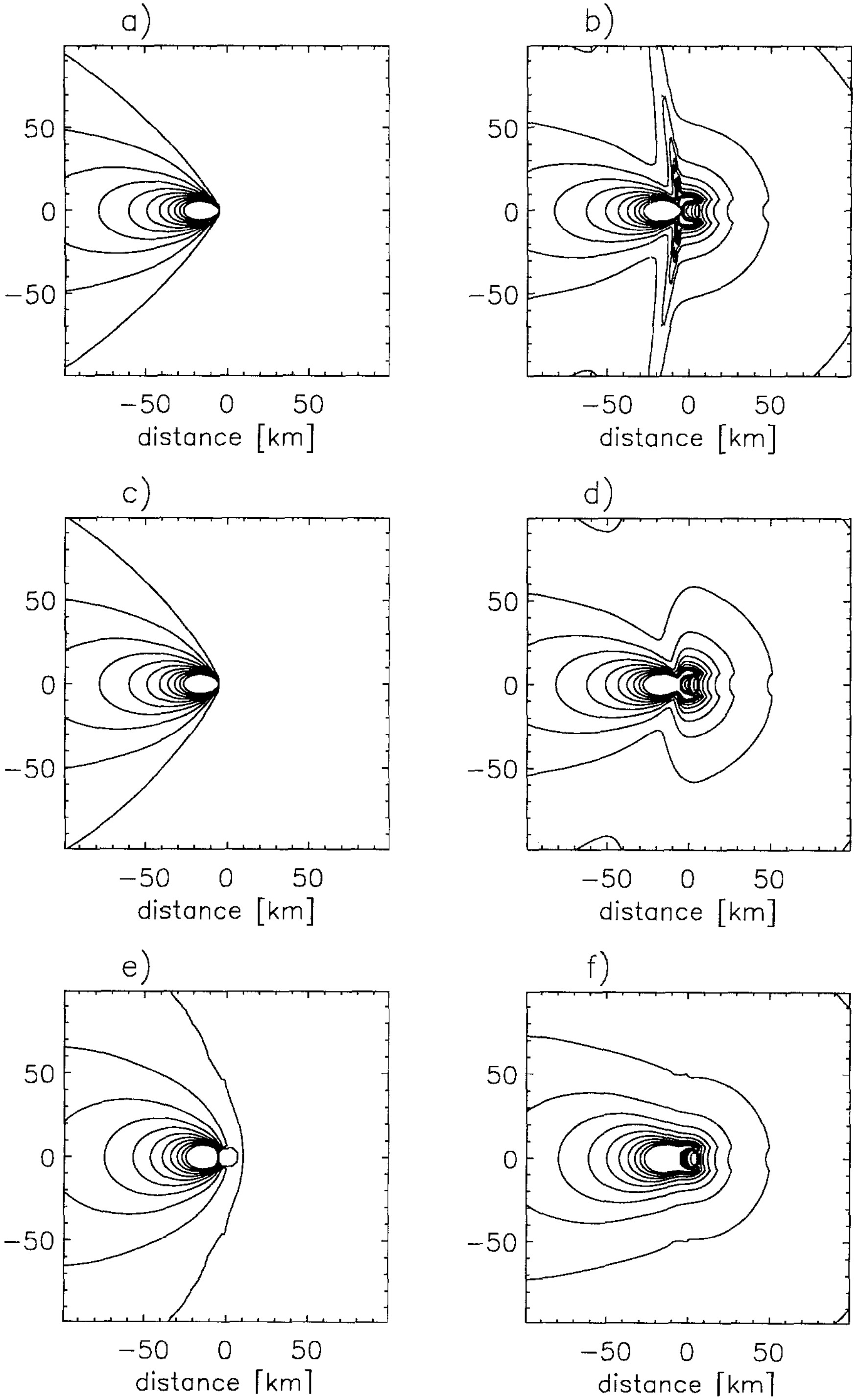


Fig. 1. Contours of intensity for different aspect angles: a), c) and e) $K_c = 0$; b), d) and f) $K_c = 0.2\ \mathrm{W\,K^{-1}\,m^{-1}}$; a), b) $\phi = 90°$; c), d) $\phi = 107°$; e), f) $\phi = 135°$

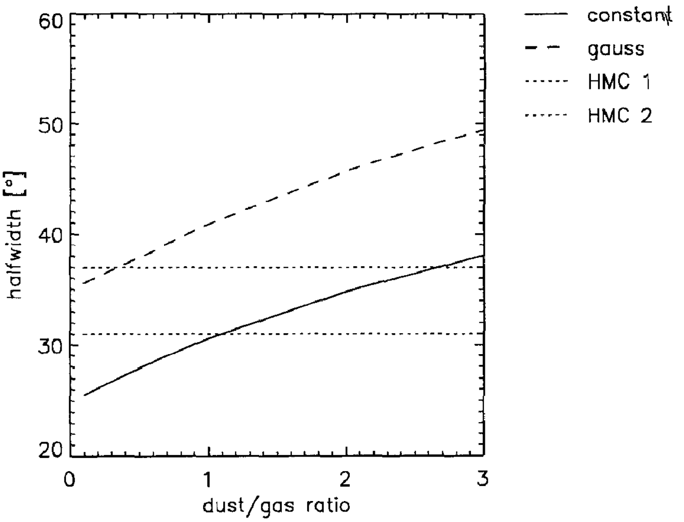


Fig. 2. Jet halfwidth as a function of the dust to gas ratio for a model with size distribution exponent $\gamma = 2.5$

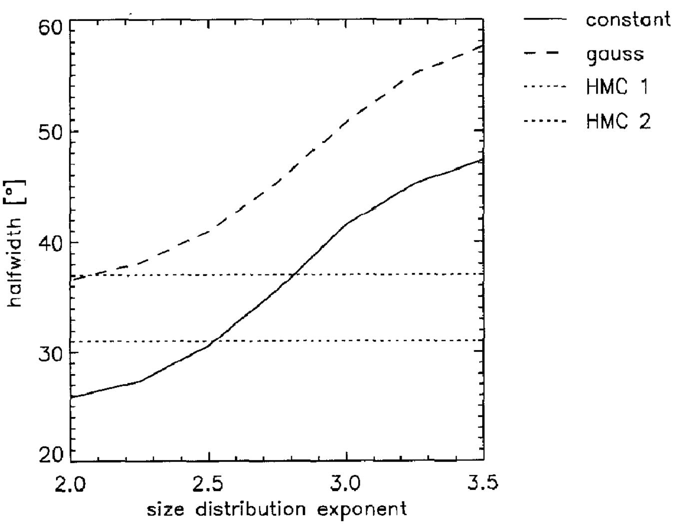


Fig. 3. Jet halfwidth as a function of the size distribution exponent $\gamma$ for a dust to gas ratio $\kappa = 1$

of these parameters is shown in Figures 2 and 3 ($\phi = 90°$). In addition, the results of another series of model runs are presented (dashed lines) where the gas and dust production inside the active area was assumed to be a Gauss function of the polar angle [$f(\Theta) = \exp(-(\Theta/\Theta_j)^2)$]. For comparison the values determined for the two strong jets visible in the HMC images are included in the plots. Because of the larger lateral pressure gradient just above the active region the Gaussian jets are in all cases about $10 - 12°$ (or 30–40%) broader than the dust jets originating from a uniformly active source. It can be seen from these figures that the most important parameter which determines the halfwidth of the jets is the distribution of grain sizes.

To conclude, Figure 4 shows a comparison of HMC data (4a) with a superposition of three axisymmetric model jets (4b) and an additional weak background (4c). The sun is to the left and 17° behind the image plane. The jets are rotated in the image plane by −43°, 15°, 85° with respect to the sun direction (counted clockwise). In the case of the southern (−43°) jet a larger active area was assumed ($\Theta_j = 20°$); therefore its total dust production is 1.8 times higher than that of the left going jet, which is again three times stronger than the weak upgoing one ($\kappa = 0.3$). The axes of the two strong jets are lying in the image plane whereas the weak northern jet is tilted by 45° out of the image plane (to the observer). It can be seen that the shape of the contours on the dayside is quite well approximated by the 3-jet model. Deviations are only significant in the vicinity of the nucleus where the irregular topography and processes like fragmentation of grains are important. But because only some dust of the weak northern jet is projected onto the nightside, the $D/N$ ratio is much higher than observed ($D/N = 15$). This discrepancy to the data can be removed by introducing a small background activity of the order of 0.2% of $Z_j$, now giving a value $D/N = 3.9$ (Fig. 4c). The slight difference in the shape of the contours on the nightside is caused by the assumed spherical shape of the model nucleus and could be removed by a more realistic approximation of the nucleus.

## 4. Discussion and Conclusions

The model calculations have shown that dust jets originating from source areas with strongly enhanced activity compared to the background develop a Gaussian shape, independent of the specific distribution of production rate inside the source region. This is in accordance with the observation of the global dust distribution in the inner coma (e.g. Keller *et al.*, 1994). Figures 2 and 3 show that the observed halfwidths of the two main jets can be explained by a model with a uniformly active region, a size distribution exponent $\gamma = 2.5 - 2.8$ and a dust to gas ratio in the range of

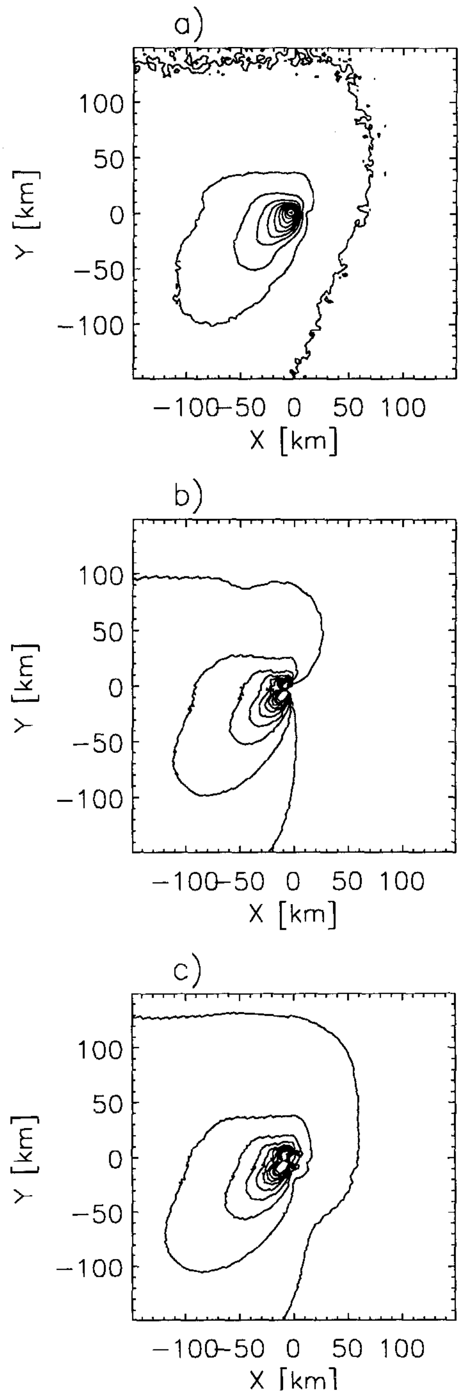


Fig. 4. Comparison of HMC data with model results: a) HMC image 3128; b) Model of three jets without background; c) Model of three jets with weak background production

$\kappa = 1 - 2.5$. This implies a grain size distribution where the mass is dominated by the larger grains, consistent with the in-situ measurements in the coma of P/Halley (McDonnell *et al.*, 1989). A size distribution with a significantly higher exponent, as deduced from optical ground based measurements [e.g. $\gamma = 3.5$ (Brin and Mendis, 1979)] would lead to much broader dust jets ($> 50°$) and, thus, cannot be representative for the coma of P/Halley at the GIOTTO encounter. The calculations presented above suggest to explain the low $D/N$-ratio observed by an approximately isotropic weak background production of gas and dust from the "inactive" areas. The background production needed is of the order of 0.1–0.3% of the free sublimation rate, a value provided by thermal models with reasonable thermal conductivities of the dust crust. In addition, such a low production rate is within the observational constraint given by the ratio of the lowest intensity measured above the nightside of the nucleus $I_c$ to the maximum intensity $I_{max}$ inside an active region of $I_c/I_{max} = 0.01$. Furthermore, it seems to be unlikely that the projection of a jet directed to or away from HMC could contribute much to the observed intensity on the nightside. First, the halfwidth of the jets increase with the deviation from $\phi = 90°$ giving values within the range of the observations only for $\phi = 90° \pm 35°$ and, second, the jump in intensity across the nightside limb would not be compatible with the observed $I_\infty/I_c = 2 - 2.5$ for $\phi > 110°$. In addition, the shape of the contours changes significantly, if the axes of the two main jets are more than 30° out of the image plane. In contrast, the dust emission of the weak and broad upgoing jet seems to be tilted with respect to the image plane. This could provide the observed halfwidth without the need of an increased dust loading and could serve as an explanation of the observed intensity gradient above the nucleus in the north-south direction (Keller and Thomas, 1989).

This analysis of the global distribution of dust in the inner coma of P/Halley therefore supports an inhomogeneous comet nucleus model where a few ice dominated active areas are surrounded by regions covered by a porous dust crust which chokes the activity to quite low values.

## References

Brin, G.D. and Mendis, D.A.: 1979, Dust release and mantle development in comets, *Astrophys. J.* **229**, 402–408.

Chick, M.K. and Gombosi, T.I.: 1992, Multiple Scattering of Light in a Spherical Shell Cometary Atmosphere with an Axisymmetric Jet, *Icarus* **98**, 179–194

Hayes, W.D. and Probstein, R.F.: 1959, *Hypersonic Flow Theory*, Academic Press, New York, USA.

Keller, H.U. and Thomas, N.: 1989, Evidence for near-surface breezes on comet P/Halley. *Astron. Astrophys.* **226**, L9–L12.

Keller, H.U., Arpigny, C., Barbieri, C., Bonnet, R.M., Cazes, S., Coradini, M., Cosmovici, C.B., Delamere, W.A., Huebner, W.F., Hughes, D.W., Jamar, C., Malaise, D., Reitsema, H.J., Schmidt, H.U., Schmidt, W.K.H., Seige, P., Whipple, F.L, and Wilhelm, K.: 1986, First Halley Multicolour Camera imaging results from Giotto. *Nature* **321**, 320–326.

Keller, H.U., Delamere, W.A., Huebner, W.F., Reitsema, H.J., Schmidt, H.U., Whipple, F.L., Wilhelm, K., Curdt, W., Kramm, J.R., Thomas, N., Arpigny, C., Barbieri, C., Bonnet, R.M., Cazes, S., Coradini, M., Cosmovici, C.B., Hughes, D.W., Jamar, C., Malaise, D., Schmidt, K., Schmidt, W.K.H., and Seige, P.: 1987, Comet P/Halley's nucleus and its activity. *Astron. Astrophys.* **187**, 807–823.

Keller, H.U., Knollenberg, J., and Markiewicz, W.J.: 1994, Collimation of Cometary Dust Jets and Filaments, *Plan. Sp. Sc.* **42**, 367–382.

Kitamura, Y.: 1986, Axisymmetric Dusty Gas Jet in the Inner Coma of a Comet. *Icarus* **66**, 241–257.

Kitamura, Y.: 1987, Axisymmetric Dusty Gas Jet in the Inner Coma of a Comet. II. The Case of Isolated Jets. *Icarus* **72**, 555–567.

Knollenberg, J.: 1994, Modellrechnungen zur Staubverteilung in der inneren Koma von Kometen unter spezieller Berücksichtigung der HMC-Daten der GIOTTO-Mission. Ph.D. Thesis, Georg-August Universität zu Göttingen, Göttingen, Germany.

Koppenwallner, G., Boettcher, R.D., Detleff, G., and Legge, H.: 1986, Rocket exhaust plume flow into space. ESA/ESTEC ESA-265.

Körösmezey, A. and Gombosi, T.I.: 1990, A Time-Dependent Dusty-Gas Dynamic Model of Axisymmetric Cometary Jets. *Icarus* **84**, 118–153.

Kührt, E. and H.U. Keller: 1994, The Formation of Cometary Surface Crusts. *Icarus* **109**, 121–132.

McDonnell, J.A.M., Green, S.F., Grün, E., Kissel, J., Nappo, S., Pankiewicz, G., and Perry, C.H.: 1989, In-situ exploration of the dusty coma of comet P/Halley at Giotto's encounter: flux rates and time profiles from $10^{-19}$ kg to $10^{-5}$ kg. *Adv. Space Res.* **9**, (3)277–(3)280.

Reitsema, H.J., Delamere, W.A., Williams, A.R., Boice, D.C., Huebner, W.F., and Whipple, F.L.: 1989, Dust Distribution in the Inner Coma of Comet Halley: Comparison with Models. *Icarus* **81**, 31–40.

Sagdeev, R.Z., Smith, B., Szegö, K., Larson, S., Tóth, I., Merényi, E., Avanesov, G.A., Krasikov, V.A., Shamis, V.A., and Tarnapolski, V.I.: 1987, The spatial distribution of dust jets seen during the Vega 2 flyby. *Astron. Astrophys.* **187**, 835-838.